

The Ellipticity of the Disks of Spiral Galaxies

Barbara S. Ryden

Department of Astronomy, The Ohio State University

140 W. 18th Avenue, Columbus, OH 43210

ryden@astronomy.ohio-state.edu

ABSTRACT

The disks of spiral galaxies are generally elliptical rather than circular. The distribution of ellipticities can be fit with a log-normal distribution. For a sample of 12,764 galaxies from the Sloan Digital Sky Survey Data Release 1 (SDSS DR1), the distribution of apparent axis ratios in the i band is best fit by a log-normal distribution of intrinsic ellipticities with $\ln \varepsilon = -1.85 \pm 0.89$. For a sample of nearly face-on spiral galaxies, analyzed by Andersen & Bershadsky using both photometric and spectroscopic data, the best fitting distribution of ellipticities has $\ln \varepsilon = -2.29 \pm 1.04$. Given the small size of the Andersen & Bershadsky sample, the two distributions are not necessarily inconsistent with each other. If the ellipticity of the potential were equal to that of the light distribution of the SDSS DR1 galaxies, it would produce 1.0 magnitudes of scatter in the Tully-Fisher relation, greater than is observed. The Andersen & Bershadsky results, however, are consistent with a scatter as small as 0.25 magnitudes in the Tully-Fisher relation.

Subject headings: galaxies: spiral – galaxies: photometry – galaxies: fundamental parameters

1. Introduction

The disks of spiral galaxies are not axisymmetric structures. Spiral arms are an obvious deviation from axisymmetry, as are bars within barred spiral galaxies. In addition, the overall shape of the disk may be elliptical rather than circular. The shape of a stellar disk can be roughly approximated as a triaxial spheroid with principal axes of length $a \geq b \geq c$. A typical stellar disk is relatively thin, with $\gamma \equiv c/a \ll 1$, and mildly elliptical, with $\varepsilon \equiv 1 - b/a \ll 1$. The exact distribution of ellipticities for the disks of spiral galaxies has long been a subject of debate.

Statistical statements about the distribution of ε can be made by looking at the distribution of apparent axis ratio q for a large population of spiral galaxies. Sandage, Freeman, & Stokes (1970) investigated a sample of 254 spiral galaxies from the *Reference Catalogue of Bright Galaxies* (de Vaucouleurs & de Vaucouleurs 1964). They concluded that the observed axis ratios of the spiral galaxies were consistent with their being a population of circular disks, with typical thickness $\gamma \approx 0.25$. Binney & de Vaucouleurs (1981), using data from the *Second Reference Catalogue of Bright Galaxies* (de Vaucouleurs, de Vaucouleurs, & Corwin 1976), concluded that late-type spirals were better fitted by mildly elliptical disks ($\varepsilon = 0.1$) than by perfectly circular disks. Using a sample of 13,482 spiral galaxies, Lambas, Maddox, & Loveday (1992) found that the ellipticity was reasonably well fitted by a Gaussian peaking at $\varepsilon = 0$:

$$f(\varepsilon) \propto \exp\left(-\frac{\varepsilon^2}{2\sigma_\varepsilon^2}\right), \quad (1)$$

subject to the constraint $0 \leq \varepsilon \leq 1$. The best fit was given by $\sigma_\varepsilon = 0.13$, yielding an average ellipticity of $\langle \varepsilon \rangle \approx 0.1$. The nonaxisymmetry of disks, which is signaled by a scarcity of apparently circular galaxies, has been confirmed by other photometric studies (Grosbøl 1985; Fasano *et al.* 1993; Alam & Ryden 2002).

Analyses which rely on the measured axis ratios of a large sample of galaxies have certain intrinsic shortcomings. First, they provide only a statistical statement about the distribution of disk ellipticities in the sample examined; they don't determine the axis ratio of any individual galaxy. Moreover, since these studies rely purely on photometry, they provide information about the ellipticity of the starlight emitted by the galaxy. The ellipticity measured in this way is affected by bars, eccentric rings and pseudorings, loosely wound spiral arms, and patchy star formation, and does not necessarily reflect the overall ellipticity of the potential within which the stars are orbiting. These intrinsic shortcomings are avoided by methods using both photometric and kinematic information.

Consider a disk of test particles orbiting in a potential which is elliptical in the disk plane. The closed particle orbits, when the potential ellipticity is small, will be elliptical themselves (Binney 1978). If the potential is logarithmic, producing a flat rotation curve, the ellipticity of the orbits will equal the ellipticity of the potential. If the resulting elliptical disk is seen in projection, the isophotal principal axes will be misaligned with the kinematic principal axes. (The kinematic principal axes can be defined as the axis along which the line-of-sight component of the rotation velocity is a maximum and the axis along which is zero.) Because of the misalignment, there is generally a non-zero velocity gradient along the isophotal minor axis, proportional to $\varepsilon \sin 2\phi$, where ε is the ellipticity of the potential, and ϕ is the azimuthal viewing angle measured relative to the long axis of the potential (Franx & de Zeeuw 1992). Studying the velocity field of gas at large radii, where the dark matter

should dominate the potential, typically yields $\varepsilon \sin 2\phi \lesssim 0.07$ (Schoenmakers, Franx, & de Zeeuw 1997).

By combining integral-field spectroscopy with imaging data, Andersen *et al.* (2001) were able to determine the intrinsic ellipticity for a number of disk galaxies at low inclination. Since the misalignment between the isophotal principal axes and the kinematic principal axes decreases as the inclination increases, the technique of Andersen *et al.* (2001) can only be usefully applied to galaxies with inclination $i < 30^\circ$. For a sample of 28 spiral galaxies, Andersen & Bershady (2003) found that the intrinsic ellipticities were well fitted by a log-normal distribution. The mean ellipticity of the galaxies in their sample was $\bar{\varepsilon} = 0.076$. The method of Andersen and collaborators has its own shortcomings. The sample of galaxies is relatively small. Systematic uncertainties in determining the isophotal and kinematic major axes can mask the signal produced by an elliptical disk (Barnes & Sellwood 2003). In addition, to ensure that their sample contained only galaxies with small inclination, Andersen *et al.* (2001) and Andersen & Bershady (2003) included only galaxies that appeared nearly circular, with $q \geq 0.866$. This selection bias discriminates against intrinsically highly elliptical disks, which have a relatively small probability of appearing nearly circular in projection. Thus, the true distribution of ellipticities will have a higher mean ellipticity and a larger standard deviation than the Andersen-Bershady sample.

In this paper, I combine information from the two types of analysis; the photometry-only method, which has the advantage of large sample size, and the Andersen *et al.* (2001) method, which has the advantage of including kinematic information which probes the potential more directly. In section 2, I use the measured apparent axis ratios of $\sim 12,800$ galaxies from the Sloan Digital Sky Survey Data Release 1 to make an estimate of their intrinsic disk ellipticities. In section 3, I reanalyze the disk ellipticities found by Andersen & Bershady (2003), taking into account the selection bias, to find the underlying distribution of disk ellipticities. I show that the two methods give results which are not mutually inconsistent. In section 4, I discuss the implications of the disk ellipticity; in particular, its relation to the scatter in the Tully-Fisher relation.

2. The SDSS Sample

The Sloan Digital Sky Survey (SDSS) is a digital photometric and spectroscopic survey which will cover, when completed, roughly one-quarter of the celestial sphere. Data Release 1 (DR1), issued to the astronomical community in 2003 April, consists of 2099 square degrees of imaging data in five photometric bands: u , g , r , i , and z (Fukugita *et al.* 1996; Stoughton *et al.* 2002). The data processing pipelines for DR1 (described in Stoughton *et al.* (2002)

and Abazajian *et al.* (2003)) fit two models to the two-dimensional image of each galaxy. The first model has a de Vaucouleurs profile (de Vaucouleurs 1948),

$$I(r) = I_0 \exp[-7.67(r/r_e)^{1/4}] , \quad (2)$$

which is truncated beyond $7r_e$, going smoothly to zero at $8r_e$; the model has some softening within $r_e/50$. The second model has an exponential profile,

$$I(r) = I_0 \exp[-1.68(r/r_e)] , \quad (3)$$

which is truncated beyond $3r_e$, going smoothly to zero at $4r_e$. Both models are assumed to have concentric elliptical isophotes with constant position angle φ_m and axis ratio q_m . Before each model is fitted to the data, the model is convolved with a double Gaussian fitted to the point-spread function (psf). Assessing each model with a χ^2 fit gives r_e , q_m , and φ_m for the best-fitting model, as well as $P(\text{deV})$ and $P(\text{exp})$, the likelihood associated with the best de Vaucouleurs model and the best exponential model, respectively. In addition, each candidate galaxy is fitted directly with the point-spread function, yielding $P(\text{psf})$, the likelihood associated with the psf fit.

To build a sample of disk galaxies from the SDSS DR1, I selected objects flagged as galaxies whose model fits in the r band satisfied the criteria $P(\text{exp}) > 2P(\text{deV})$ and $P(\text{exp}) > 2P(\text{psf})$. In addition, each galaxy was required to have a spectroscopic redshift $z < 0.1$, to reduce the possibility of weak lensing distorting the observed shape, and $z > 0.002$, to eliminate a few contaminating foreground objects. The spectroscopic sample of the SDSS DR1 contained 30,184 galaxies satisfying these criteria. Note that I have selected galaxies on the basis of their surface brightness profile (exponential rather than de Vaucouleurs), and not on other criteria such as color or isophote shape. It is generally true, though, that bright early-type galaxies (elliptical and S0) are better fitted by de Vaucouleurs profiles than by exponential profiles, and that spiral galaxies are better fitted by exponential profiles (Strateva *et al.* 2001). Moreover, the spectroscopic sample of the DR1 contains galaxies which are too high in surface brightness to be dwarf ellipticals, which can also have exponential surface brightness profiles (Binggeli & Cameron 1991). Thus, I will assume that the galaxies which I have chosen on the basis of their exponential profiles are disk-dominated spiral galaxies.

The model fits to the exponential galaxies provide one measure of the axis ratio q . However, a model with constant position angle φ and axis ratio q is not a good approximation to a real spiral galaxy. Fortunately, the SDSS DR1 photometric analysis also provides more robust, model-free measures of the axis ratio. One useful shape measure is q_{am} , the axis ratio determined by the use of adaptive moments. In general, the technique of adaptive moments determines the n th order moments of an image using an elliptical weight function whose shape matches that of the object (Bernstein & Jarvis 2002; Hirata & Seljak 2003).

In practice, the SDSS adaptive moments use a Gaussian weight function $w(x, y)$ which is matched to the size and ellipticity of the galaxy image $I(x, y)$. With the weight function $w(x, y)$ known, the moments can be calculated:

$$\vec{x}_0 = \frac{\int \vec{x} w(x, y) I(x, y) dx dy}{\int w(x, y) I(x, y) dx dy} , \quad (4)$$

$$M_{xx} = \frac{\int (x - x_0)^2 w(x, y) I(x, y) dx dy}{\int w(x, y) I(x, y) dx dy} , \quad (5)$$

and so forth. The SDSS DR1 provides for each image the adaptive second moments

$$T = M_{xx} + M_{yy} , \quad (6)$$

$$e_+ = (M_{xx} - M_{yy})/T , \quad (7)$$

and

$$e_\times = 2M_{xy}/T . \quad (8)$$

The adaptive second moments can be converted into an axis ratio using the relation

$$q_{\text{am}} = \left(\frac{1 - e}{1 + e} \right)^{1/2} , \quad (9)$$

where $e \equiv (e_+^2 + e_\times^2)^{1/2}$. The adaptive moments axis ratio computed in this way are not corrected for the effects of seeing. However, the SDSS DR1 also provides the adaptive second moments, T_{psf} , $e_{+, \text{psf}}$, and $e_{\times, \text{psf}}$, for the point spread function at the location of the image. These moments can be used to correct for the smearing and shearing due to seeing; such corrections are vital in studying the small shape changes resulting from weak lensing (Bernstein & Jarvis 2002; Hirata & Seljak 2003). However, to eliminate the need for corrections, I will only retain galaxies which are well resolved, with $r_e > 5\sqrt{T_{\text{psf}}}$. Of the five bands used by SDSS, the g , r , and i bands provide useful morphological information; the low detector sensitivity at u and z and the high background at z make them less useful for study. At g , $N_{\text{gal}} = 12,826$ galaxies satisfy my criteria, at r , the number is $N_{\text{gal}} = 12,751$, and at i , it's $N_{\text{gal}} = 12,764$.

Because the weight function $w(x, y)$ is scaled to the size of the galaxy image, the adaptive moments axis ratio q_{am} can be thought of as an average axis ratio to which the outer regions of the galaxy, beyond the effective radius, do not contribute significantly. The shape in the outer region can be found from the shape of the 25 magnitude per square arcsecond isophote. The SDSS DR1 provides, for each galaxy in each band, the values of a_{25} and b_{25} , the long and short semimajor axis length for the isophote at the surface brightness 25 mag/arcsec². The isophotal axis ratio $q_{25} \equiv b_{25}/a_{25}$ then provides a measure of the galaxy shape in its

outer regions. The mean and standard deviation of a_{25}/r_e for the galaxies in examined in this paper is 2.12 ± 0.56 in the g band, 2.56 ± 0.72 in the r band, and 2.82 ± 0.84 in the i band. Having two different measures of the axis ratio, q_{am} and q_{25} , thus allows comparison of the central shape (q_{am}) and the outer shape (q_{25}). Having measures in three different bands, g , r , and i , gives some information about the wavelength dependence of the disks' apparent ellipticity. The i band, having the longest wavelength of those studied, will be least affected by dust and by patches of star formation.

The distribution of q_{am} , in the i band, is shown as the histogram in Figure 1. The relative scarcity of nearly circular galaxies is the characteristic signature of nonaxisymmetry. To fit the observed distribution of apparent axis ratios, I adopted a model in which the disk thickness γ has a Gaussian distribution,

$$f(\gamma) \propto \exp \left[-\frac{(\gamma - \mu_\gamma)^2}{2\sigma_\gamma^2} \right] \quad (10)$$

subject to the constraint $0 \leq \gamma \leq 1$, and the disk ellipticity ε has a log-normal distribution,

$$f(\varepsilon) \propto \frac{1}{\varepsilon} \exp \left[-\frac{(\ln \varepsilon - \mu)^2}{2\sigma^2} \right] , \quad (11)$$

subject to the constraint $\ln \varepsilon \leq 0$. After assuming values for the four parameters μ_γ , σ_γ , μ , and σ , a chi-square fit to the data in Figure 1 can be made. I randomly selected a thickness γ and ellipticity ε from the distributions in equations 10 and 11. I then randomly selected a viewing angle (θ, ϕ) and computed the resulting apparent axis ratio (Binney 1985)

$$q = \left[\frac{A + C - \sqrt{(A - C)^2 + B}}{A + C + \sqrt{(A - C)^2 + B}} \right]^{1/2} , \quad (12)$$

where

$$A = [1 - \varepsilon(2 - \varepsilon) \sin^2 \varphi] \cos^2 \theta + \gamma^2 \sin^2 \theta , \quad (13)$$

$$B = 4\varepsilon^2(2 - \varepsilon)^2 \cos^2 \theta \sin^2 \varphi \cos^2 \varphi , \quad (14)$$

$$C = 1 - \varepsilon(2 - \varepsilon) \cos^2 \varphi . \quad (15)$$

By repeating this procedure $N_{\text{gal}} = 12,764$ times, I created one realization of the μ_γ , σ_γ , μ , σ parameter set. After creating 16,000 realizations, I computed the mean and standard deviation of the expected number of galaxies in each of the 40 bins in Figure 1, and computed a χ^2 probability for that particular set of parameters. A search through four-dimensional parameter space revealed that the best fit for q_{am} in the i band was provided by the set of parameters $\mu_\gamma = 0.222$, $\sigma_\gamma = 0.057$, $\mu = -1.85$, and $\sigma = 0.89$. The resulting χ^2 probability

was $P = 3 \times 10^{-4}$. Formally, this is not a good fit to the data, but more than half the contribution to χ^2 comes from the bins on the far left, with $q_{\text{am}} < 0.3$. As emphasized by Fasano *et al.* (1993), the distributions of γ and ε for spiral galaxies are almost completely decoupled, in that the distribution of γ determines the left hand side of $f(q)$ while the distribution of ε determines the right hand side. The model’s relatively poor fit at $q_{\text{am}} < 0.3$ indicates that the galaxies in the sample have a distribution of thicknesses which is not well fit by a Gaussian. In any case, the distribution of disk thicknesses in my sample is not the same as the true distribution of disk thicknesses. As shown by Huizinga & van Albada (1992), a magnitude-limited sample of galaxies such as the SDSS DR1 spectroscopic galaxy sample, which has a limiting (Petrosian) magnitude $r < 17.77$, will show a deficit of high-inclination, low- q spiral galaxies. This deficit is due to extinction by dust. In the B band, for instance, an Sc galaxy is 1 to 1.5 magnitudes fainter when seen edge-on than when seen face-on (Huizinga & van Albada 1992). Although the inclination-dependent dimming is smaller at longer wavelengths and for earlier type spirals, the fitted disk thickness should be regarded with skepticism. Fortunately for the purposes of this paper, spiral galaxies that appear nearly circular ($q \gtrsim 0.8$) are nearly face-on, and hence their thickness is almost totally irrelevant; it’s the distribution of disk ellipticity ε that determines the shape of $f(q)$ at large q .

Table 1 shows the best fitting model parameters, μ_γ , σ_γ , μ , and γ , for the two different shape measures, q_{am} and q_{25} , and for the three different bands, g , r , and i . In addition, the best values of μ and γ are plotted as points in Figure 2. Note that going from g band (triangles) to r band (squares) to i band (circles) results in a smaller spread of disk ellipticities (that is, smaller values of σ). Going from q_{am} (filled symbols) to q_{25} (open symbols) results in a smaller disk ellipticity (that is, smaller values of μ). In the i band, for instance, using q_{am} for the shape measure results in a best fit log-normal distribution with $\mu = -1.85$ and $\sigma = 0.89$; the modal ellipticity for this distribution is 0.071, the median is $\approx e^\mu \approx 0.16$, and the mean is 0.21. Using q_{25} for the shape measure results in $\mu = -2.06$ and $\sigma = 0.83$; the modal ellipticity is 0.064, the median is $\approx e^\mu \approx 0.13$, and the mean is 0.17. Although the disks are rounder, on average, in the outer regions, they still have a significant ellipticity. Note also the color dependence of the mean thickness μ_γ ; galactic disks are thicker, on average, at longer wavelengths. This dependence reflects the fact that older stellar populations, which have redder colors, have a greater vertical velocity dispersion and hence a greater disk scale height (Wielen 1977; Dehnen & Binney 1998).

The large SDSS DR1 sample of galaxies places strong constraints on the best fitting values of μ and σ . To demonstrate how the goodness of fit varies in (μ, σ) parameter space, Figure 2 shows the isoproability contours for the q_{am} data in the i band. Note that the contours are drawn at an interval of $\Delta \log_{10} P = 2$; the χ^2 probability drops rapidly as you

move away from the best fit, indicated by the filled circle at the center of the innermost contour. At other wavelengths, and using the other shape measure q_{25} , the probability falls off with comparable steepness in (μ, σ) parameter space.

The log-normal distribution of equation (11) is not the only functional form to yield an adequate fit to the data. A Gaussian peaking at $\varepsilon = 0$, as shown in equation (1), provides a comparably good fit to the SDSS DR1 data. In the i band, the best-fitting Gaussian to the q_{am} data has $\sigma_\varepsilon = 0.26$. The best-fitting Gaussian to the q_{25} data has $\sigma_\varepsilon = 0.21$. The photometry provided by the SDSS DR1 is insufficient to distinguish between a Gaussian distribution of ellipticities, peaking at $\varepsilon = 0$, and a log-normal distribution, peaking at $\varepsilon > 0$. Purely photometric studies, it seems, are ill-suited to addressing the question of whether exactly circular disks, with $\varepsilon = 0$, exist.

3. The Andersen-Bershady Sample

Andersen & Bershady (2003), using the method outlined in Andersen *et al.* (2001), combined kinematic and I -band photometric data to find the disk ellipticity for a sample of 28 nearly face-on disk galaxies; the mean inclination of the galaxies is $i = 26^\circ$. The distribution of $\ln \varepsilon$ determined by Andersen & Bershady (2003) is shown as the histogram in Figure 3. This distribution is well fitted by a log-normal distribution; the best fit, as found by a χ^2 test, has parameters $\mu = -2.80$ and $\sigma = 0.81$. However, the best fit to the data in Figure 3 is not the best fit to the underlying distribution of disk ellipticities, thanks to the selection criteria used in building the sample. To ensure that only galaxies with small inclination were included, Andersen & Bershady (2003) selected galaxies with $q \geq 0.866$, corresponding to an inclination $i \leq 30^\circ$ for perfectly circular, infinitesimally thin disks.

To fit the distribution of intrinsic ellipticities in the Andersen-Bershady sample, subject to their selection criterion $q \geq 0.866$, I started by assuming that the disk ellipticity has the log-normal form given in equation (11). I further assumed, for simplicity, that the disks are all infinitesimally thin; since the disks in the Andersen-Bershady sample are close to face-on, their exact thickness doesn't affect the observed axis ratio. After assuming values for the parameters μ and σ , I randomly selected a disk ellipticity ε as well as a viewing angle (θ, ϕ) . If the resulting apparent axis ratio, as given by equation (12), was $q \leq 0.866$, I retained it in my sample. If it was flatter than this limit, I discarded it. By repeating this procedure until I had $N_{\text{gal}} = 28$ axis ratios, I created one possible realization. After creating 16,000 realizations, I computed the mean and standard deviation in each of the bins in Figure 3. A search through parameter space revealed that the best fit, as measured by a χ^2 test, was given by $\mu = -2.29$, $\sigma = 1.04$. The probability of the fit, illustrated by the points and error

bars in Figure 3, was $P = 0.98$.

The 28 galaxies of Andersen & Bershady (2003) do not, by themselves, provide a strong constraint on the distribution of intrinsic ellipticities. Figure 4 shows the goodness of fit, as measured by the χ^2 probability $P_{AB}(\mu, \sigma)$. The cross indicates the best fit, and the dotted and solid lines show the isoprobability contours. Note that the $P = 0.1$ contour – the innermost dotted line – encloses a large area stretching off to the upper right of the plot. That is, a distribution with a large value of μ , corresponding to a very flattened average shape, is acceptable as long as it is paired with a large value of σ , signifying a wide spread in shapes. Because the Andersen-Bershady contains only galaxies which are nearly circular in projection, it is strongly weighted toward galaxies which are nearly circular in their intrinsic shape, and thus cannot effectively constrain the high-ellipticity end of $f(\varepsilon)$.

A Gaussian peaking at $\varepsilon = 0$ (see equation (1)) doesn't provide a good fit to the Andersen-Bershady sample. The best-fitting Gaussian, with $\sigma_\varepsilon = 0.143$, had a χ^2 probability of only $P = 0.009$. Thus, although the data of Andersen & Bershady (2003) doesn't constrain the high-ellipticity end of $f(\varepsilon)$, its discriminatory power at low values of ε weighs strongly against a distribution peaking at $\varepsilon = 0$.

The kinematic and photometric information exploited by Andersen & Bershady (2003) is in some ways complementary to the purely photometric information included in the SDSS DR1 axis ratios. The nearly face-on galaxies of the Andersen-Bershady sample constrain the low-ellipticity end of $f(\varepsilon)$; the scarcity of nearly circular galaxies in the SDSS DR1 exponential sample (see Figure 1) constrains the high-ellipticity end of $f(\varepsilon)$. The kinematic measurements of Andersen *et al.* (2001) typically go out to $2 \rightarrow 3$ scale lengths ($1.2 \rightarrow 1.8r_e$). The ellipticities determined by Andersen *et al.* (2001) and Andersen & Bershady (2003) can be thought of as average ellipticities over the inner region of the galaxy. Thus, the Andersen-Bershady ellipticities are more directly comparable to the ellipticities found from q_{am} than from the outer axis ratios q_{25} . As shown in Figure 4, the best fit using q_{am} in the i band, indicated by the filled circle, is marginally consistent with the Andersen-Bershady results. Multiplying together the probability fields in Figure 2 and Figure 4 yields a best joint fit of $\mu = -1.89$, $\sigma = 0.96$. For this set of parameters, the χ^2 fit to the Andersen-Bershady data has $P = 0.44$, and the fit to the q_{am} data in the i band has $P = 9.5 \times 10^{-5}$.

4. Discussion

In this paper, I've considered two quite different ways of determining disk ellipticities. The SDSS DR1 axis ratios are a measure of where the starlight is in a galaxy, and hence

contain information about bulges, bars, spiral arms, and other nonaxisymmetric structure in the galaxies. By its nature, the analysis of photometric axis ratios finds difficulty in distinguishing between a Gaussian distribution of ellipticities peaking at $\varepsilon = 0$ and a log-normal distribution peaking at $\varepsilon > 0$. If you want to determine whether truly circular disks actually exist, examining the apparent axis ratios of disks (even of a large number of disks) is not an effective method to use. By contrast, the approach of Andersen *et al.* (2001) and Andersen & Bershadsky (2003) uses both photometric and kinematic information to find the ellipticity of individual disks. Since Andersen & Bershadsky (2003) looked at disks which are nearly circular in projection, their data are ineffective at determining the high-ellipticity end of $f(\varepsilon)$.

Although both data sets are reasonably well fitted by a log-normal distribution with $\ln \varepsilon = -1.89 \pm 0.96$, this distribution should not be engraved on stone as *the* distribution of disk ellipticities in spiral galaxies. Describing a complex structure such as a spiral galaxy with a single number ε (or even two numbers, ε and γ) requires averaging over a great deal of substructure. How one takes the average will affect the value of ε found. For instance, using the adaptive moments shape q_{am} yields larger values for the ellipticity than using the isophotal shape q_{25} . Moreover, observations at different wavelengths result in different values of ε .

If a disk of gas and stars is orbiting in a logarithmic potential which is mildly elliptical in the disk plane, with $\varepsilon_\phi \ll 1$, then the integrated line profile from the disk will have a width $W = 2v_c(1 - \varepsilon_\phi \cos 2\varphi) \sin \theta$ when viewed from a position angle φ, θ (Franx & de Zeeuw 1992). The alteration in the line width, due to noncircular motions in the elliptical potential, will produce a scatter in the observed Tully-Fisher relation between line width and absolute magnitude (Tully & Fisher 1977). For an ellipticity $\varepsilon_\phi = 0.1$, the expected scatter is 0.3 magnitudes (Franx & de Zeeuw 1992). (This assumes that the inclination has been determined accurately using kinematic information; if the inclination is determined photometrically, assuming the disk is circular, there will be an additional source of scatter.)

If the potential ellipticity ε_ϕ is assumed to be drawn from a log-normal distribution, and the embedded disk is viewed from a random angle, the resulting scatter in the Tully-Fisher relation is shown in Figure 5. The best fits for the SDSS DR1 data are superimposed as triangles (*g* band), squares (*r* band) and circles (*i* band). Even in the *i* band, the best fit to the ellipticity of the disks would produce far more scatter than is seen in the Tully-Fisher relation. Using q_{am} as the shape measure (as shown by the filled circle in Figure 5), 1.0 magnitude of scatter is predicted. Using q_{25} as the measure (as shown by the open circle in Figure 5), 0.8 magnitudes of scatter is predicted. The best fit to the Andersen-Bershadsky data, shown as the cross in Figure 5, would also produce 0.8 magnitudes of scatter in the

Tully-Fisher relation.

In contrast, the actual scatter in the Tully-Fisher relation is smaller than 0.8 magnitudes. Courteau (1997) found 0.46 magnitudes of scatter in the optical Tully-Fisher relation when he used, as his velocity measure, the rotation speed at 2.2 scale lengths ($\sim 1.3r_e$), about the extent of the kinematic data of Andersen *et al.* (2001). Verheijen (2001), in his study of spiral galaxies in the Ursa Major cluster, found still smaller scatters. Combining near-infrared K' magnitudes with V_{flat} , the rotation speed in the outer, flat part of the rotation curve, Verheijen (2001) found a best fit with zero intrinsic scatter, with an upper limit, at the 95% confidence level, of 0.21 magnitudes.

The SDSS DR1 data are clearly inconsistent with such small scatters in the Tully-Fisher relation. The light distribution in the i band cannot reflect the ellipticity of the underlying potential, but must be due primarily to nonaxisymmetric structures such as bars, spiral arms, non-circular rings, and so forth. It should be noted that lopsidedness ($m = 1$ distortions) is not uncommon in disk galaxies; Rix & Zaritsky (1995) found that a third of the galaxies in their sample of nearly face-on spirals had significant lopsidedness at 2.5 scale lengths ($\sim 1.5r_e$). Unfortunately, the SDSS DR1 does not provide, among its tabulated parameters, the odd moments that would permit a quantitative estimate of disk lopsidedness.

Although barred galaxies were excluded from the Andersen-Bershady sample, I made no effort to sift out barred galaxies from my SDSS DR1 sample. The Andersen-Bershady results are not inconsistent with a small scatter in the Tully-Fisher relation. The dashed line in Figure 5 is the $P = 0.5$ contour for the Andersen-Bershady sample; that is, every (μ, σ) pair within the dashed line gives a “too-good-to-be-true” fit to the sample of Andersen & Bershady (2003). This contour encloses (μ, σ) pairs which produce as little as 0.32 magnitudes of scatter. At lower probability levels, the $P = 0.1$ contour yields as little as 0.28 magnitudes and the $P = 0.01$ contour yields as little as 0.25 magnitudes of scatter. In summary, the Andersen-Bershady data are consistent with as little as a quarter-magnitude of scatter in the Tully-Fisher relation. The Andersen-Bershady data are also consistent with the adaptive moments axis ratios from the SDSS DR1. However, the three sets of information – the Andersen-Bershady data, the Tully-Fisher scatter (or lack thereof), and the SDSS DR1 axis ratios – are not mutually consistent. The SDSS DR1 axis ratios, if they accurately traced the potential ellipticity, would produce too much scatter in the Tully-Fisher relation.

I thank Matt Bershady, Dave Andersen, Richard Pogge, and Albert Bosma for their helpful and courteous comments. Ani Thakar was an invaluable guide to the sdssQA query tool. The Sloan Digital Sky Survey (SDSS) is a joint project of The University of Chicago, the Institute of Advanced Study, the Japan Participation Group, the Max-Planck-Institute for

Astronomy (MPIA), the Max-Planck-Institute for Astrophysics (MPA), New Mexico State University, Princeton Observatory, the United States Naval Observatory, and the University of Washington. Apache Point Observatory, site of the SDSS telescopes, is operated by the Astrophysical Research Consortium (ARC). Funding for the project has been provided by the Alfred P. Sloan Foundation, the SDSS member institutions, the National Aeronautics and Space Administration, the National Science Foundation, the U.S. Department of Energy, the Japanese Monbukagakusho, and the Max Planck Society. The SDSS website is <http://www.sdss.org/>.

REFERENCES

- Abazajian, K., et al. 2003, *AJ*, in press (astro-ph/0305492)
- Alam, S. M. K., & Ryden, B. S. 2002, *ApJ*, 570, 610
- Andersen, D. R., & Bershady, M. A. 2003, in *Disks of Galaxies: Kinematics, Dynamics, and Perturbations*, ed. E. Athanassoula & A. Bosma
- Andersen, D. R., Bershady, M. A., Sparke, L. S., Gallagher, J. S., & Wilcots, E. M. 2001, *ApJ*, 551, L131
- Barnes, E. I., & Sellwood, J. A. 2003, *AJ*, 125, 1164
- Bernstein, G. M., & Jarvis, M. 2002, *AJ*, 123, 583
- Binggeli, B., & Cameron, L. M. 1991, *A&A*, 252, 27
- Binney, J. 1978, *MNRAS*, 183, 779
- Binney, J. 1985, *MNRAS*, 212, 767
- Binney, J., & de Vaucouleurs, G. 1981, *MNRAS*, 194, 679
- Courteau, S. 1997, *AJ*, 114, 2402
- Dehnen, W., & Binney, J. J., 1998, *MNRAS*, 298, 387
- de Vaucouleurs, G. 1948, *Ann. d’Astrophys.*, 11, 247
- de Vaucouleurs, G., & de Vaucouleurs, A. 1964, *Reference Catalogue of Bright Galaxies*, U. Texas Press, Austin

- de Vaucouleurs, G., de Vaucouleurs, A., & Corwin, H. G. 1976, Second Reference Catalogue of Bright Galaxies, U. Texas Press, Austin
- Fasano, G., Amico, P., Bertola, F., Vio, R., & Zeilinger, W. W. 1993, MNRAS, 262, 109
- Franx, M., & de Zeeuw, T. 1992, ApJ, 392, L47
- Fukugita, M., Ichikawa, T., Gunn, J. E., Doi, M., Shimasaku, K., & Schneider, D. P. 1996, AJ, 111, 1748
- Grosbøl, P. J. 1985, A&AS, 60, 261
- Hirata, C., & Seljak, U. 2003, MNRAS, 343, 459
- Huizinga, J. E., & van Albada, T. S. 1992, MNRAS, 254, 677
- Lambas, D. G., Maddox, S. J., & Loveday, J. 1992, MNRAS, 258, 404
- Rix, H.-W., & Zaritsky, D. 1995, ApJ, 447, 82
- Sandage, A., Freeman, K. C., & Stokes, N. R. 1970, ApJ, 160, 831
- Schoenmakers, R. H. M., Franx, M., & de Zeeuw, P. T. 1997, MNRAS, 292, 349
- Stoughton, C., et al. 2002, AJ, 123, 485
- Strateva, I., et al. 2001, AJ, 122, 1861
- Tully, R. B., & Fisher, J. R. 1977, A&A, 54, 661
- Verheijen, M. A. W. 2001, ApJ, 563, 694
- Wielen, R. 1977, A&A, 60, 263

Table 1. Best Fitting Models: Gaussian Thickness Distribution, Log-normal Ellipticity Distribution

Shape Measure	Band	N_{gal}	$\mu_{\gamma} \pm \sigma_{\gamma}$	$\mu \pm \sigma$	P_{χ^2}
Adaptive moments (q_{am})	g	12,826	0.205 ± 0.054	-1.79 ± 1.01	5×10^{-5}
	r	12,751	0.216 ± 0.056	-1.83 ± 0.93	5×10^{-4}
	i	12,764	0.222 ± 0.057	-1.85 ± 0.89	3×10^{-4}
25 mag/arcsec ² isophote (q_{25})	g	12,826	0.211 ± 0.056	-2.03 ± 1.09	2×10^{-2}
	r	12,751	0.231 ± 0.064	-2.07 ± 0.96	3×10^{-3}
	i	12,764	0.248 ± 0.074	-2.06 ± 0.83	2×10^{-6}
Andersen-Bershady	I	28		-2.29 ± 1.04	0.996

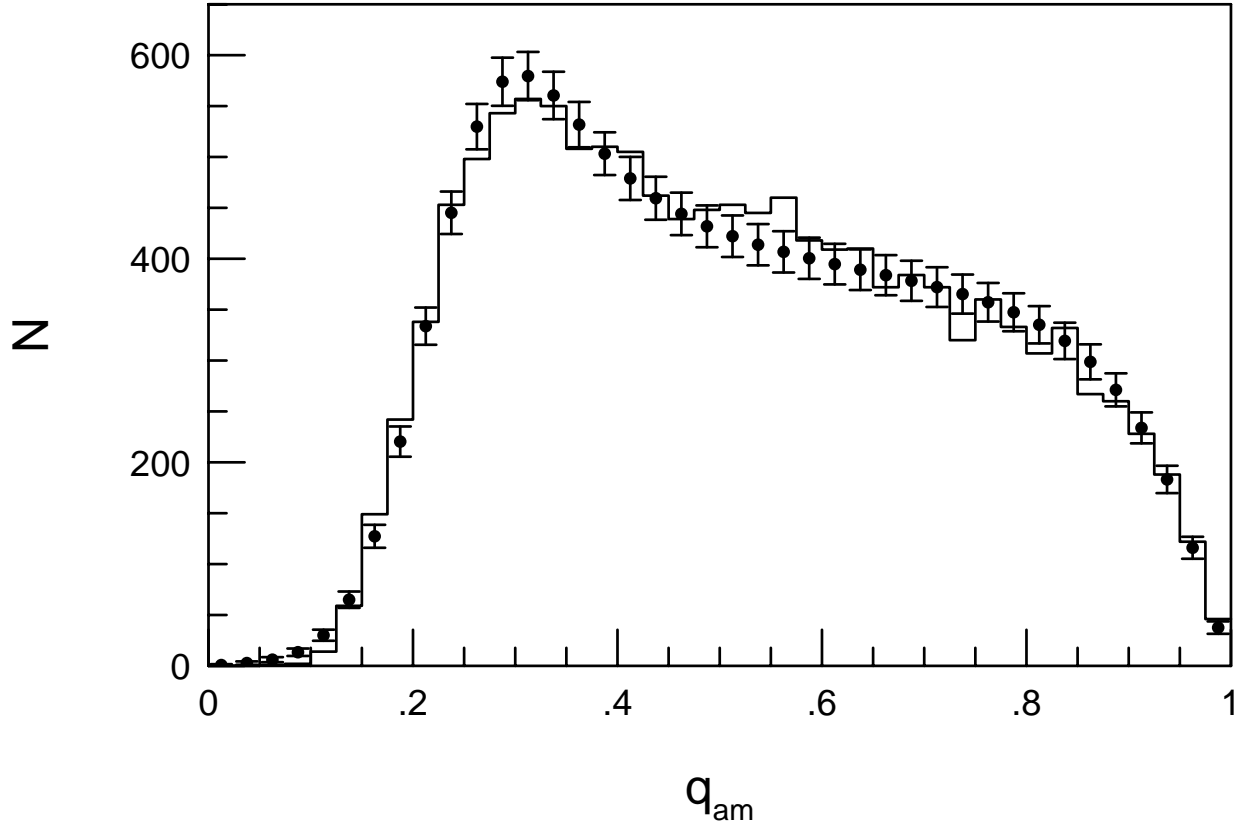


Fig. 1.— Histogram: the distribution of axis ratio q_{am} , using adaptive moments in the i band, for exponential galaxies in the SDSS DR1. Points with error bars: the best fitting model, assuming a Gaussian distribution of disk thickness and a log-normal distribution of intrinsic disk ellipticity. The best fitting model has thickness $\gamma = 0.222 \pm 0.057$ and ellipticity $\ln \varepsilon = -1.85 \pm 0.89$.

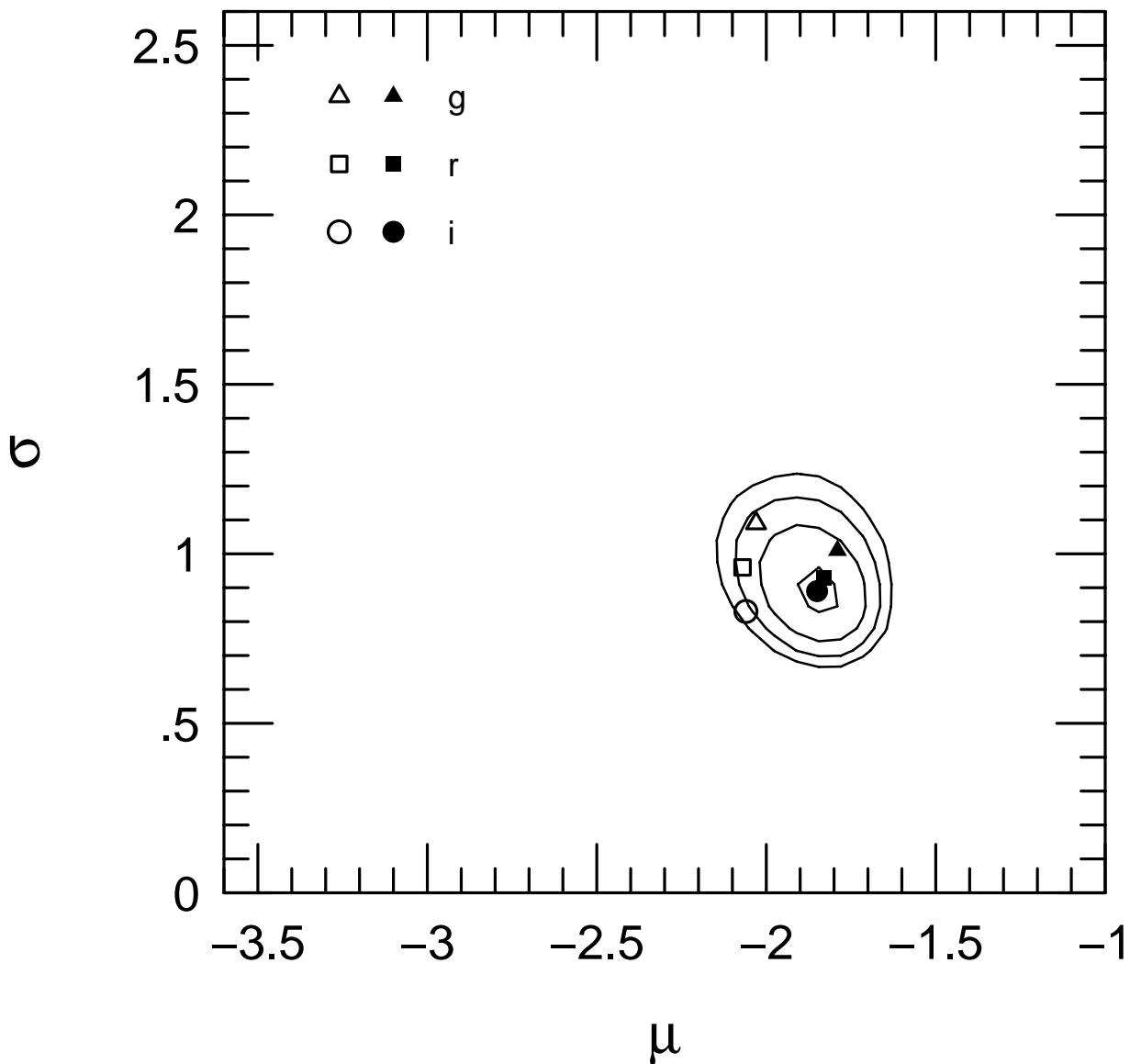


Fig. 2.— The points indicate the best fitting values of μ and σ , assuming a log-normal distribution of intrinsic disk ellipticities. Open symbols use q_{25} , the axis ratio of the 25 mag/arcsec² isophote, for the apparent shape measure; filled symbols use q_{am} , the adaptive moments axis ratio, for the apparent shape measure. The solid lines are isoproability contours, as measured by a χ^2 test applied to the binned data of Figure 1. Contours are drawn at the levels $\log_{10} P = -4, -6, -8,$ and -10 , going from the innermost to outermost contour.

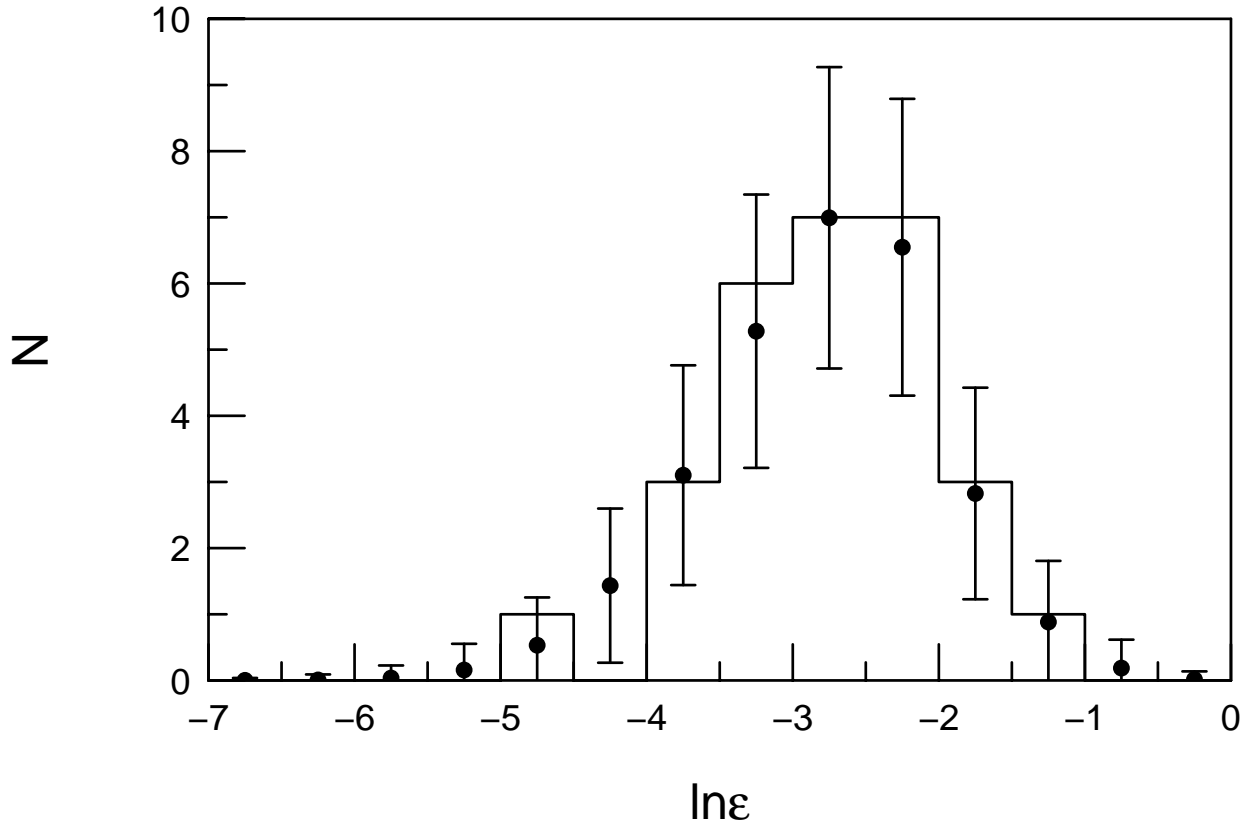


Fig. 3.— Histogram: the distribution of $\ln \varepsilon$ for the Andersen-Bershady sample of galaxies. Points with error bars: the best fitting model, assuming a log-normal distribution of intrinsic disk ellipticity. The best fitting parent distribution has $\ln \varepsilon = -2.29 \pm 1.04$. (If the selection criterion $q \geq 0.866$ were ignored, the best fit would have $\ln \varepsilon = -2.80 \pm 0.81$.)

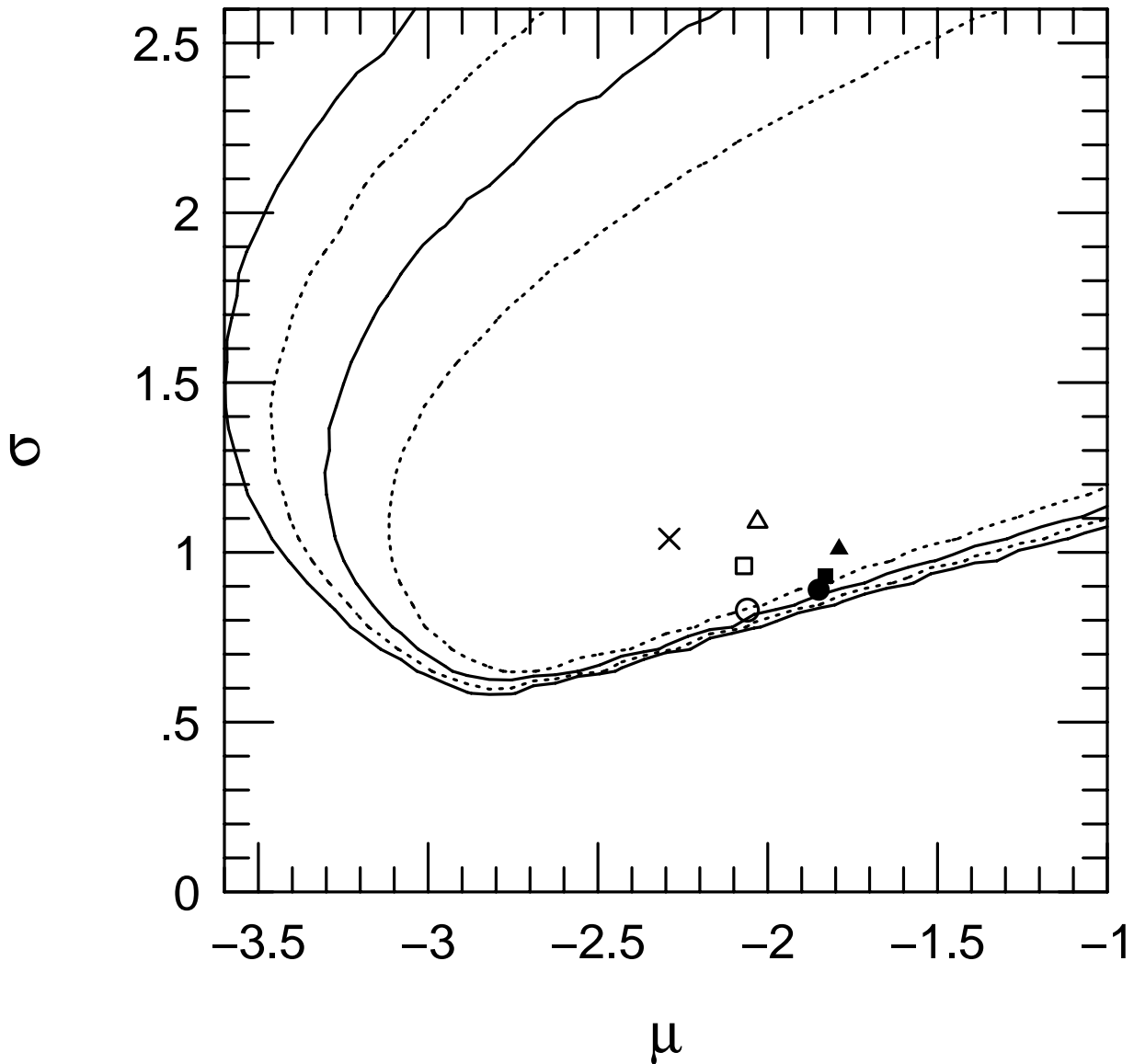


Fig. 4.— Isoprobability contours, as measured by a χ^2 test applied to the binned data of Figure 3, in (μ, σ) parameter space. Contours are drawn at the levels $\log_{10} P = -1, -2, -3,$ and -4 , going from the innermost to outermost contour. The cross indicates the best fit: $\mu = -2.29, \sigma = 1.04$. The best fitting points for the SDSS DR1 data are repeated from Figure 2, for comparison purposes.

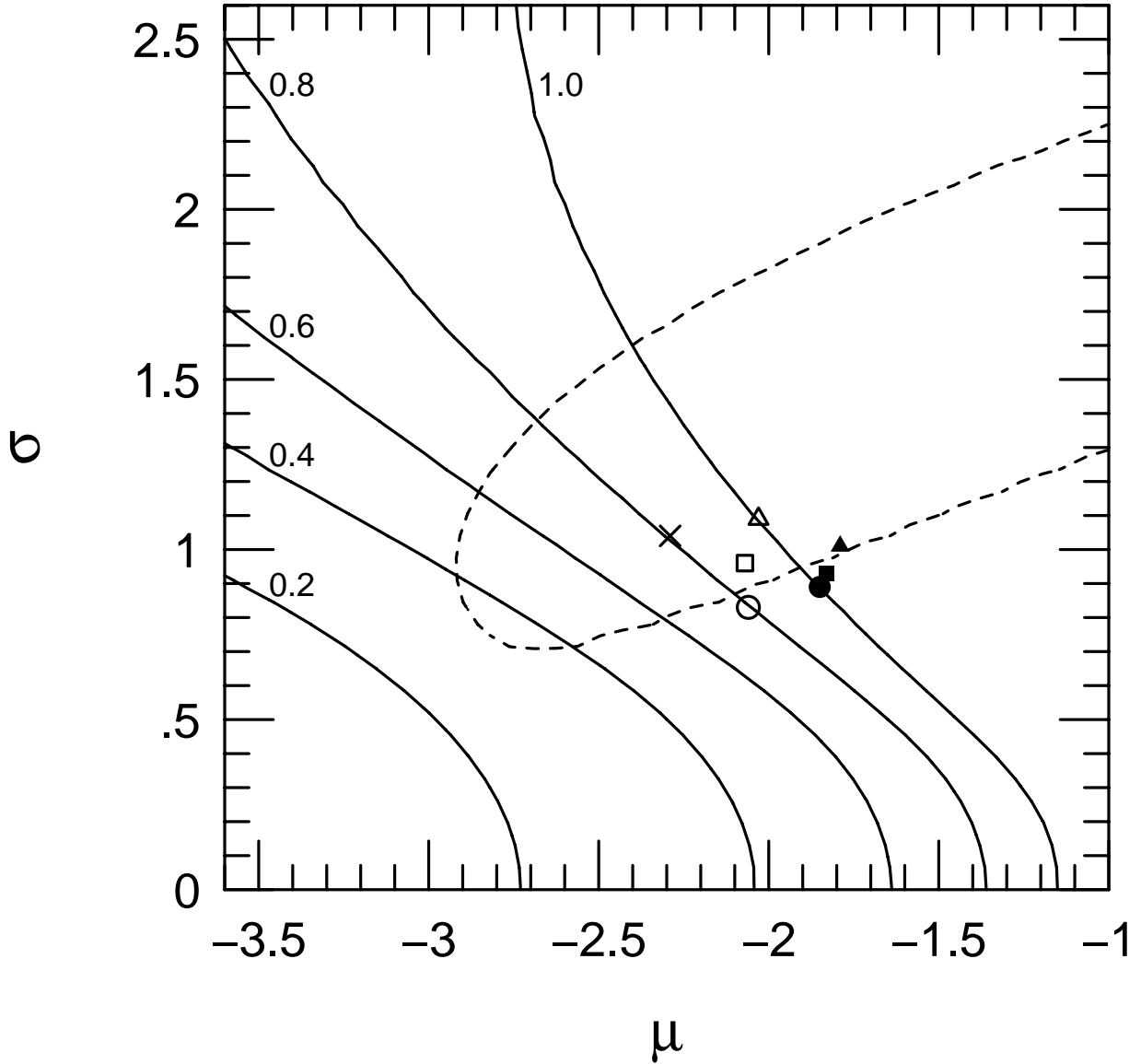


Fig. 5.— The scatter, in magnitudes, around the mean Tully-Fisher relation, for a log-normal distribution of potential ellipticity. The contours are drawn, starting at the lower left, at the levels 0.2, 0.4, 0.6, 0.8, and 1.0 magnitudes. The dashed line indicates the 50% probability contour for the Andersen-Bershady data. The cross is the best fit for the Andersen-Bershady data. The open and filled symbols are the best fits for the SDSS DR1 data, repeated from Figure 2.